J. Fluid Mech. (1982), *vol.* 123, *pp.* 219–236
Printed in Great Britain

The boundary layer on a fixed sphere on the axis of an unbounded rotating fluid

By S. C. R. DENNIS
Department of Applied Mathematics, University of Western Ontario, London, Canada

AND D. B. INGHAM
Department of Applied Mathematical Studies, University of Leeds, England

(Received 23 June 1981 and in revised form 23 March 1982)

The problem of determining both the steady and unsteady axially symmetrical motion of a viscous incompressible fluid outside a fixed sphere when the fluid at large distances rotates as a solid body is considered. It is assumed that the Reynolds number for the motion is so large that the boundary-layer equations may be assumed to hold. The steady-state boundary-layer equations are solved using backward–forward differencing and the terminal solutions at the equator and the pole of the sphere are generated as part of the numerical procedure. To check that this steady-state solution can be approached from an unsteady situation, the case of a sphere that is initially rotating with the same constant angular velocity as the fluid and is then impulsively brought to rest is investigated. In this case the motion is governed by a coupled set of three nonlinear time-dependent partial differential equations, which are solved by employing the semi-analytical method of series truncation to reduce the number of independent variables by one and then solving by numerical methods a finite set of partial differential equations in one space variable and time. The physical properties of the flow are calculated as functions of the time and compared with the known solution at small times and the steady-state solution.

1. Introduction

The steady flow of a viscous fluid due to a sphere that rotates about a diameter with constant angular velocity in a fluid at rest has received much attention theoretically, experimentally and numerically. Recently Dennis, Ingham & Singh (1981) have reviewed this work and shown that their numerical solutions for values of the Reynolds number R ($= a^2\omega_0/\nu$, where a is the radius of the sphere, ω_0 its angular velocity and ν the coefficient of kinematic viscosity of the fluid) up to 5000 are in excellent agreement with the experimental results of Sawatzki (1970) and theoretical results valid at small values of the Reynolds number given by Takagi (1977). At large values of the Reynolds number the results appear to be approaching the boundary-layer solution given, for example, by Banks (1976) everywhere except near the equator of the sphere. Here there is evidence of the development of the equatorial jet in which fluid near the sphere is drawn towards the equator and expelled in a radial jet in a region close to the equator. This phenomenon has been observed experimentally by Bowden & Lord (1963). At large distances from the sphere the radial jet is in good agreement with that predicted by Riley (1962) and observed experimentally by Richardson (1976). In the range of Reynolds number of the numerical solutions no evidence was found to substantiate the theoretical prediction of Smith & Duck (1977) that a recirculating region exists near the sphere in the equatorial region.

In this paper the inverse of the above problem is considered, namely the flow due to a fixed sphere in a uniformly rotating fluid with the sphere centred on the axis of rotation. Stewartson (1957) postulated that the sphere could create a local disturbance for $R \gg 1$, and applied boundary-layer theory, taking the outer boundary condition to be that of uniform rotation. He used a Pohlhausen method to solve the boundary-layer equations with the same approximation that Howarth (1951) had previously applied in the rotating-sphere problem. Stewartson conjectured that the flow at the poles of the sphere is of the form given by Bödewadt (1940). In the vicinity of the equator he obtained a similarity-type solution. Thus the fluid is drawn into the boundary layer near the equator and expelled near the poles, there being none left inside the boundary layer at the poles.

The earliest example to be considered of flow due to a solid object at rest in a rotating fluid was in fact that due to a circular disk of radius a. An approximate solution using the momentum integrals was given by Schultz-Grünow (1935), and he found that the boundary layer begins at the edge of the disk and its thickness is virtually proportional to $(a-r)^{\frac{1}{2}}$, where r denotes the distance from the axis of the disk, which is the axis of rotation. The boundary layer spreads over the whole disk, but the convergence of the series expansions used by Schultz-Grünow were not satisfactory near $r = 0$.

The problem of the flow in the boundary layer due to a free vortex, with the azimuthal velocity proportional to r^{-1}, on a fixed co-axial disk has been solved by Burggraf, Stewartson & Belcher (1971). Using the similarity solution that is valid near the edge of the disk, the boundary-layer equations were integrated numerically for decreasing values of r until the properties of the terminal solution became evident. A two-layer asymptotic expansion was formulated for the solution of the boundary-layer equations near $r = 0$, and the terminal-flow properties revealed by the analysis were shown to be in excellent agreement with the numerical results. The mass flux in the boundary layer did not vanish as $r \to 0$, thus indicating that the boundary layer must erupt from the surface at $r = 0$ in the manner envisioned by Moore (1956). The numerical calculations can, however, be continued step by step from the edge of the disk to any predetermined non-zero value of r.

The work of Burggraf *et al.* (1971) was extended by Belcher, Burggraf & Stewartson (1972) to deal with the situation where the outer flow is a generalized vortex with the azimuthal velocity proportional to r^{-n}, where $-1 \leqslant n \leqslant 1$. The case $n = 1$ had already been discussed by the same three authors, and when $n = -1$ the problem considered reduces to that discussed by Cooke (1966) and Anderson (1966). In the case $n = -1$ there are sign reversals in the radial component of velocity, which implies that a numerical solution cannot be obtained by marching step by step in a radial direction because of instabilities. Surprisingly, Anderson was able to obtain a solution down to 40% of the disk radius. Because of the possibility of non-uniqueness and instabilities of the previous methods Belcher *et al.* (1972) used a time-dependent approach. They found it impracticable to compute the solution right up to $r = 0$ so they considered the possibility of obtaining solutions for $r_E \leqslant r \leqslant 1$, where r_E is a sufficiently small value of r such that the terminal solution as $r \to 0$ can be inferred from knowledge of the solution near r_E. However, a solution in $r_E \leqslant r \leqslant 1$ is not uniquely determined by the conditions on the disk, in the free stream and at the edge of the disk, since we can apply arbitrary conditions on that part of the line $r = r_E$ where $u < 0$. This is because disturbances travel with the local velocity and hence move outwards if $u > 0$. Thus a change in boundary condition on $r = r_E$ where $u > 0$ would modify the flow in the region of interest, i.e. $r_E \leqslant r \leqslant 1$, whereas if the change

of boundary condition were made where $u < 0$ then the solution in $r_E \leqslant r \leqslant 1$ would be unaffected. This kind of phenomenon has received much attention recently, and has been discussed in detail by Ingham (1978). The first successful methods of solution were given by Hall (1969) and Dennis (1972). Belcher *et al.* (1972) followed Hall's method by introducing time as an additional variable, and they carried out the integration forward in time until the solution was judged to be steady. It was noted that this steady-state criterion was not always easy to enforce since the solution may change very slowly with time.

In the present paper the problem corresponding to $n = -1$ but with a sphere rather than a disk has been considered, i.e. the boundary-layer solution is determined for a fixed sphere on the axis of an unbounded fluid that is rotating as a solid body at large enough distances. The consideration of the case of a sphere rather than a disk eliminates the need for taking account of the singular solution that exists at the edge of the disk. Further, the terminal solutions are obtained from the numerical computations rather than by using an enforced boundary condition as in the disk problem. The method of solution used is similar to that of Dennis (1972) rather than Hall (1969), since this eliminates the difficulties of judging when the flow is steady. Banks (1971) obtained the first three non-zero terms in the series expansion for the solution to this problem that is valid near the equator of the sphere, and the first two non-zero terms in the expansion valid near the pole. In attempting to obtain higher-order terms his analysis suggested that the effect of the sphere is not a local one but rather the flow is of the Taylor-column type. He produced experimental evidence that confirmed the existence of this phenomenon. Thus one of the aims of the present paper is to discover if a steady-state solution of the boundary-layer equations is possible for this situation, although physically this may not be achieved. We may note that in the rather similar situation arising in the problem of flow in a curved pipe at large Dean number, Smith (1975) has obtained a similarity solution valid near the inner bend of the pipe, but could not match this with the similarity solution near the outer bend.

The question that then arises is whether, even if a steady-state boundary-layer solution does exist, this can be attained from an unsteady situation. This is not always possible in this type of problem, as Bodonyi (1978) discovered when considering the unsteady similarity equations for the flow above a rotating disk in a rotating fluid. He considered the unsteady similarity equations for a large rotating disk immersed in an otherwise unbounded rigidly rotating incompressible fluid for several values of the parameter α that denotes the ratio of the angular velocity of the disk to that of the rigidly rotating fluid. He found in a particular range of α that although steady-state solutions exist, the unsteady solutions broke down at a finite value of the time. In these cases it was found that either velocity components became infinite or that limit cycle solutions existed. Banks & Zaturska (1979) confirmed in general the findings of Bodonyi. In particular, both investigations showed that the approach to the steady-state situation is very slow when $\alpha = 0$; this case corresponds to the flow near the pole of the sphere in the present problem.

In the light of these difficulties, it was decided in the present paper to consider in more detail the unsteady approach to the solution that is valid near the equator by using techniques similar to those described by both Bodonyi (1978) and Banks & Zaturska (1979). Further, the full unsteady boundary-layer equations have been integrated numerically using the series-truncation method described by Dennis & Ingham (1979). In that paper an investigation was made of the fluid flow due to suddenly starting a sphere rotating with a constant angular velocity. The boundary-layer

equations were integrated up to a certain time, beyond which the number of terms required in the series expansions became excessive and it was impossible to retain enough terms to maintain a high degree of accuracy. This was mainly due to the formation of the equatorial jet. At the time at which the calculations were terminated all quantities had almost settled down to their steady values everywhere except near the equator. In the present paper the reverse of the problem considered by Dennis & Ingham (1979) is considered, namely the sphere and fluid are assumed to be in solid-body rotation and then the sphere is suddenly brought to rest. When the sphere is stopped suddenly a boundary layer of thickness proportional to $t^{\frac{1}{2}}$ is initially formed on the surface. Therefore at small times the unsteady boundary-layer equations are solved numerically with the appropriate scaling in the radial direction. After the initial growth of the boundary layer has been accounted for one reverts back to the normal boundary-layer coordinates and the equations are solved for increasing values of time.

2. Basic equations

Non-dimensional spherical polar coordinates (ar, θ, ϕ) with corresponding velocity components $a\omega_0(w, u, v)$ are used, where a is the radius of the sphere, ω_0 the angular velocity of the fluid at large distances, $r = 0$ is the centre of the sphere and $\theta = 0$ is the axis of rotation of the fluid. On assuming the flow to be axially symmetric (i.e. $\partial/\partial\phi \equiv 0$) then the equations of motion and continuity in the form given by Banks (1971) are

$$\frac{\partial w}{\partial t}+w\frac{\partial w}{\partial r}+\frac{u}{r}\frac{\partial w}{\partial \theta}-\frac{u^2+v^2}{r}=-\frac{\partial p}{\partial r}+\frac{1}{R}\left[\nabla^2 w-\frac{2w}{r^2}-\frac{2}{r^2}\frac{\partial u}{\partial \theta}-\frac{2u\cot\theta}{r^2}\right], \tag{1}$$

$$\frac{\partial u}{\partial t}+w\frac{\partial u}{\partial r}+\frac{u}{r}\frac{\partial u}{\partial \theta}+\frac{uw-v^2\cot\theta}{r}=-\frac{1}{r}\frac{\partial p}{\partial \theta}+\frac{1}{R}\left[\nabla^2 u+\frac{2}{r^2}\frac{\partial w}{\partial \theta}-\frac{u}{r^2\sin^2\theta}\right], \tag{2}$$

$$\frac{\partial v}{\partial t}+w\frac{\partial v}{\partial r}+\frac{u}{r}\frac{\partial v}{\partial \theta}+\frac{vw+uv\cot\theta}{r}=\frac{1}{R}\left[\nabla^2 v-\frac{v}{r^2\sin^2\theta}\right], \tag{3}$$

$$\frac{1}{r^2}\frac{\partial}{\partial r}(r^2 w)+\frac{1}{r\sin\theta}\frac{\partial}{\partial \theta}(u\sin\theta)=0, \tag{4}$$

where

$$\nabla^2=\frac{1}{r^2}\frac{\partial}{\partial r}\left(r^2\frac{\partial}{\partial r}\right)+\frac{1}{r^2\sin\theta}\frac{\partial}{\partial \theta}\left(\sin\theta\frac{\partial}{\partial \theta}\right), \tag{5}$$

$$R=a^2\omega_0/\nu \tag{6}$$

and the pressure has been non-dimensionalized with respect to $\rho a^2\omega_0^2$.

Equations (1)–(4) have to be solved subject to the boundary conditions

$$u=v=w=0 \quad (r=1), \tag{7}$$

$$u, w\to 0, \quad v\to r\sin\theta \quad (r\to\infty), \tag{8}$$

and in the unsteady configuration the conditions are

$$\left.\begin{aligned} &u=w=0, \quad v=r\sin\theta \quad (r\geqslant 1, t<0),\\ &v=0, \quad (r=1, t\geqslant 0). \end{aligned}\right\} \tag{9}$$

3. Steady boundary-layer equations

If $R \gg 1$ then, following Stewartson (1957), we assume that away from the surface of the sphere the flow is described approximately by the inviscid solution $u = w = 0$, $v = r\sin\theta$, but that near $r = 1$ there is a boundary layer in which the radial derivative of a given quantity is much greater than the corresponding derivative in the θ-direction. A balance of the inertial and viscous terms in the boundary layer suggests the introduction of the stretched radial coordinate z given by

$$z = (r-1)R^{\frac{1}{2}}. \tag{10}$$

If we now perform the usual boundary-layer analysis, putting $w = R^{-\frac{1}{2}}\tilde{w}$ in (1)–(4) and then dropping the tilde, they become

$$w\frac{\partial u}{\partial z} + u\frac{\partial u}{\partial \theta} - \Omega^2\frac{\cos\theta}{\sin^3\theta} = -\sin\theta\cos\theta + \frac{\partial^2 u}{\partial z^2}, \tag{11}$$

$$w\frac{\partial \Omega}{\partial z} + u\frac{\partial \Omega}{\partial \theta} = \frac{\partial^2 \Omega}{\partial z^2}, \tag{12}$$

$$\frac{\partial w}{\partial z} + \frac{\partial u}{\partial \theta} + u\cot\theta = 0, \tag{13}$$

$$p = \tfrac{1}{2}\sin^2\theta. \tag{14}$$

The boundary conditions for these equations are

$$u = v = w = 0 \quad (z = 0), \tag{15}$$

$$u \to 0, \quad \Omega \to \sin^2\theta \quad (z \to \infty). \tag{16}$$

Here $\Omega = v\sin\theta$, which is the function used by Dennis *et al.* (1981). Also, by symmetry of the motion we have that

$$u = \Omega = \frac{\partial w}{\partial \theta} = 0 \quad (\theta = 0), \tag{17}$$

$$u = \frac{\partial \Omega}{\partial \theta} = \frac{\partial w}{\partial \theta} = 0 \quad (\theta = \tfrac{1}{2}\pi). \tag{18}$$

Because of the symmetry it is only necessary to obtain a solution in the region $0 \leqslant \theta \leqslant \frac{1}{2}\pi$ and $0 \leqslant z \leqslant z_\infty$, where z_∞ is the station at which the flow may be assumed to be undisturbed. In this region a rectangular grid is set up with nodes at the points

$$\left.\begin{aligned} z_i &= (i-1)h \quad (i = 1, 2, 3, \ldots, M+1), \\ \theta_j &= (j-1)k \quad (j = 1, 2, 3, \ldots, N+1), \end{aligned}\right\} \tag{19}$$

where $M = z_\infty/h$, $N = \pi/2k$, and h, k are the grid sizes in the z- and θ-directions.

The partial differential equations (11)–(13) are now discretized using central differences everywhere except for the terms involving $\partial u/\partial\theta$ in (11) and $\partial\Omega/\partial\theta$ in (12), where forward or backward differences are used according to the sign of the coefficient u of these terms. The differencing is therefore of second-order accuracy in h but only of first-order accuracy in k, and the approximations are generally less accurate than if central differences were used throughout. The advantage is that the matrices associated with the sets of difference equations are diagonally dominant. This type of method was used by Dennis (1972) in a similar class of problems; and it has been

used with much success in many other problems. Thus the resulting finite-difference equations to be solved are

$$(1-\tfrac{1}{2}hw_{i,j})\,u_{i+1,j}+(1+\tfrac{1}{2}hw_{i,j})\,u_{i-1,j}\pm\gamma q_{i,j}u_{i,j\mp1}+h^2\Omega_{i,j}^2\cos\theta_j/\sin^3\theta_j - h^2\sin\theta_j\cos\theta_j=(2\pm\gamma q_{i,j})\,u_{i,j}, \quad (20)$$

$$(1-\tfrac{1}{2}hw_{i,j})\,\Omega_{i+1,j}+(1+\tfrac{1}{2}hw_{i,j})\,\Omega_{i-1,j}\pm\gamma q_{i,j}\Omega_{i,j\mp1}=(2\pm\gamma q_{i,j})\,\Omega_{i,j}, \quad (21)$$

$$w_{i+1,j}=w_{i,j}-\tfrac{1}{2}h\cot\theta_j\,(u_{i,j}+u_{i+1,j})-\frac{h}{4k}(u_{i,j+1}-u_{i,j-1}+u_{i+1,j+1}-u_{i+1,j-1}), \quad (22)$$

where $q_{i,j}=u_{i,j}$, $\gamma=h^2/k$, and the upper signs apply when $u_{i,j}>0$ and the lower signs when $u_{i,j}<0$.

It is this procedure of ensuring that the diagonal coefficient $2\pm\gamma q_{i,j}$ of each of the matrices associated with the sets of equations (20) and (21) is in effect replaced by $2+\gamma|u_{i,j}|$ that preserves diagonal dominance and leads to convergent iterative procedures. Equation (22) is obtained by applying the Crank–Nicolson procedure to (13), considered as a first-order equation in the z-direction. Equations (20)–(22) must be solved for $i=2,3,\ldots M$ and $j=2,3,\ldots,N$. The values of w on $\theta=0$ and Ω and w on $\theta=\frac{1}{2}\pi$ are found by using the finite-difference equation (22) on $\theta=0$ and $\theta=\frac{1}{2}\pi$ and (21) on $\theta=\frac{1}{2}\pi$, using symmetry conditions where appropriate. The position of the outer boundary at $z=z_\infty$ was varied and a value $z_\infty=18$ was found to be satisfactory. Four different grids were used corresponding to values of (M,N) given by $(40,20)$, $(80,40)$, $(100,50)$ and $(120,60)$. The results obtained with the last two of these grids were indistinguishable graphically.

In order to start the iterative process all unknown quantities were set to zero. The correct sequence of procedures is of considerable importance, and, moreover, simply setting $q_{i,j}=u_{i,j}$ and taking, say, the positive sign always in (20) and (21) resulted in divergence. The iterative sequence, which converged without using under-relaxation, was as follows.

(i) Fix w, Ω and q while one sweep of (20) is carried out. In this sweep the grid points are swept along lines of constant θ, whilst in the z-direction the sweeps were made in the decreasing z-direction for $0\leqslant\theta\leqslant\frac{1}{4}\pi$ and in the increasing z-direction for $\frac{1}{4}\pi<\theta\leqslant\frac{1}{2}\pi$. This takes account of the fact that the similarity solution at the poles must be obtained by marching towards $z=0$ and that at the equator by marching away from $z=0$.

(ii) Fix w, u and q while one sweep of (21) is carried out in the same order as that described in (i).

(iii) Fix u while one sweep of (22) is carried out in the same order as that described in (i).

(iv) Set q equal to u.

(v) Perform steps (i)–(iv) until convergence. This was said to have been achieved when

$$\Sigma\,|f_{i,j}^{(n+1)}-f_{i,j}^{(n)}|<\epsilon, \quad (23)$$

where f is w, Ω and u, and the summation extends to all grid points. The quantity ϵ is a predetermined constant of small positive value. In the present calculations $\epsilon=10^{-4}$ was found to be small enough.

Banks (1971) solved the equations (11)–(13) by assuming that

$$\left.\begin{aligned} u=\sum_{n=0}^{\infty}(\theta-\tfrac{1}{2}\pi)^{2n+1}F_{2n+1}(z), \quad v=\sum_{n=0}^{\infty}(\theta-\tfrac{1}{2}\pi)^{2n}G_{2n+1}(z),\\ w=\sum_{n=0}^{\infty}(\theta-\tfrac{1}{2}\pi)^{2n}H_{2n+1}(z) \end{aligned}\right\} \quad (24)$$

near $\theta = \frac{1}{2}\pi$. On substituting the expressions (24) into equations (11)–(13) and equating coefficients of powers of $\theta - \frac{1}{2}\pi$ three sets of ordinary differential equations were obtained, which were solved numerically for $F_{2n+1}, G_{2n+1}, H_{2n+1}$ $(n = 0, 1, 2)$. The approach to the polar solution was obtained by expanding the velocity components about $\theta = 0$, where the leading term is simply the Bödewadt similarity solution. In this region the expansion is

$$u = \sum_{n=0}^{\infty} \theta^{2n+1} F_{2n}(z), \quad v = \sum_{n=0}^{\infty} \theta^{2n+1} G_{2n}(z), \quad w = \sum_{n=0}^{\infty} \theta^{2n} H_{2n}(z). \tag{25}$$

Again substituting the expressions (25) into (11)–(13) and equating coefficients of powers of θ Banks obtained three sets of ordinary differential equations, which were solved for F_{2n}, G_{2n} and H_{2n} $(n = 0, 1)$. These calculations were repeated in the present investigation and the results obtained by Banks (1971) confirmed.

In figures 1 and 2 the variation of the skin-friction components $R^{-\frac{1}{2}}(\partial u/\partial r)_{r=1}$ and $R^{-\frac{1}{2}}(\partial v/\partial r)_{r=1}$ are shown from results obtained by the numerical solution of the finite-difference equations (20)–(22). Also shown are the leading terms of the solutions in the forms of the expansions (24) and (25). In this case

$$\left.\begin{aligned} R^{-\frac{1}{2}}(\partial u/\partial r)_{r=1} &\sim -0{\cdot}94197\theta + 0{\cdot}34100\theta^3 \\ R^{-\frac{1}{2}}(\partial v/\partial r)_{r=1} &\sim 0{\cdot}77288\theta - 0{\cdot}30367\theta^3 \end{aligned}\right\} \quad \text{near} \quad \theta = 0; \tag{26}$$

$$\left.\begin{aligned} R^{-\frac{1}{2}}(\partial u/\partial r)_{r=1} &\sim 0{\cdot}95389(\theta - \tfrac{1}{2}\pi) - 0{\cdot}50911(\theta - \tfrac{1}{2}\pi)^3 \\ &\qquad + 0{\cdot}03955(\theta - \tfrac{1}{2}\pi)^5 \\ R^{-\frac{1}{2}}(\partial v/\partial r)_{r=1} &\sim 0{\cdot}46154 - 0{\cdot}10752(\theta - \tfrac{1}{2}\pi)^2 \\ &\qquad + 0{\cdot}00123(\theta - \tfrac{1}{2}\pi)^4 \end{aligned}\right\} \quad \text{near} \quad \theta = \tfrac{1}{2}\pi. \tag{27}$$

It is seen that the results of taking successively more terms in (26) and (27) are consistent with those of the numerical solutions of (20)–(22).

Figure 3 shows the variation of the radial velocity at the outer edge of the boundary layer $w(\theta, \infty)$. Also shown are the leading terms from (24) and (25), which are given by

$$\left.\begin{aligned} w(\infty, \theta) &\sim 1{\cdot}349 - 0{\cdot}189\theta^2 \quad \text{near} \quad \theta = 0, \\ w(\infty, \theta) &\sim -1{\cdot}3284 + 3{\cdot}2756(\theta - \tfrac{1}{2}\pi)^2 + 1{\cdot}5041(\theta - \tfrac{1}{2}\pi)^4 \quad \text{near} \quad \theta = \tfrac{1}{2}\pi. \end{aligned}\right\} \tag{28}$$

It was found that even with a very crude grid size and the value of z_∞ as small as 10, the results presented in figures 1 and 2 for the solution of the finite-difference equations (20)–(22) could be obtained correct to within a few per cent. On the other hand, the value of $w(\theta, \infty)$ is very sensitive to the values of h, k and z_∞. The sensitivity to the size of h and k is probably due to the rapid variation of $w(\theta, \infty)$ near $\theta = \frac{1}{4}\pi$, and if insufficient grid points are used in the θ-direction the finite-difference equations cannot approximate adequately these gradients. This results in the terminal solution near $\theta = 0$ not being approached smoothly but in an oscillatory manner; oscillations are in fact present in the final solutions. The large gradients of the solutions, particularly $w(\theta, \infty)$, near $\theta = \frac{1}{4}\pi$ could be dealt with by employing a non-uniform grid in the θ-direction; but in any case great care has been taken to ensure that the grid is small enough to obtain accurate solutions.

In order to demonstrate the approach to the solutions at $\theta = 0$ and $\frac{1}{2}\pi$ more fully, figures 4 and 5 show the transverse velocity profiles at $\theta = \frac{1}{20}\pi, \frac{1}{10}\pi, \frac{1}{5}\pi, \frac{1}{4}\pi$ and $\theta = \frac{9}{20}\pi, \frac{2}{5}\pi, \frac{3}{10}\pi, \frac{1}{4}\pi, \frac{1}{5}\pi$ respectively. Also shown in figures 4 and 5 are u/θ and $u/(\frac{1}{2}\pi - \theta)$,

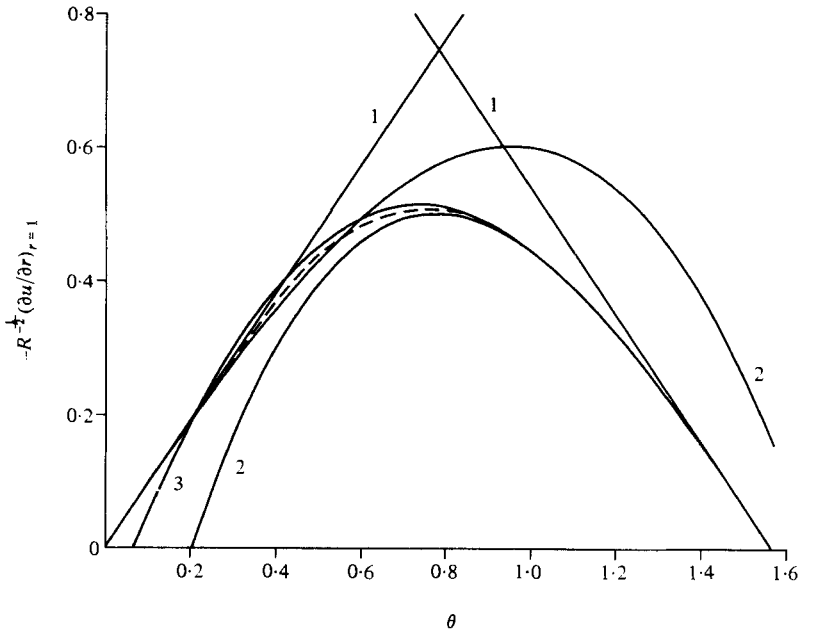

FIGURE 1. The variation of $R^{-\frac{1}{2}}(\partial u/\partial r)_{r=1}$ as a function of θ. The numbers 1, 2 and 3 indicate the number of terms used in (26) and (27). The broken line is the numerical solution.

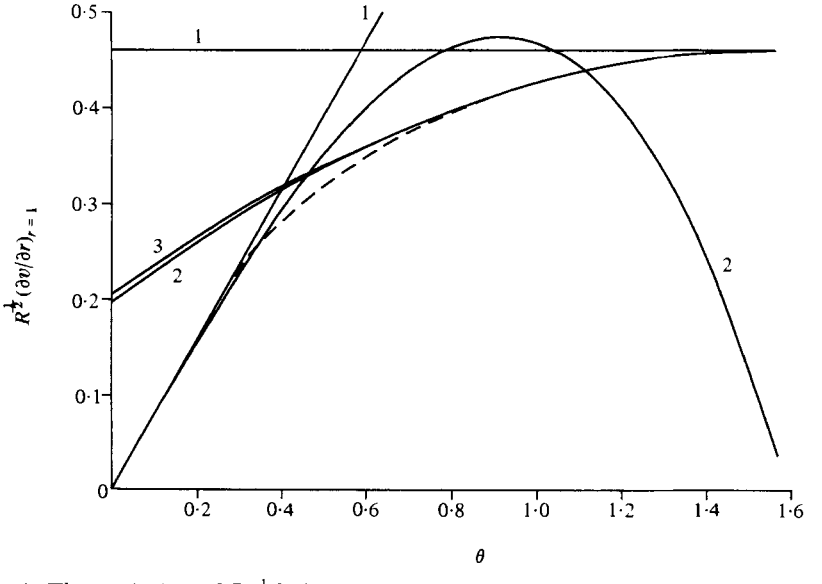

FIGURE 2. The variation of $R^{-\frac{1}{2}}(\partial v/\partial r)_{r=1}$ as a function of θ. The numbers 1, 2 and 3 indicate the number of terms used in (26) and (27). The broken line is the numerical solution.

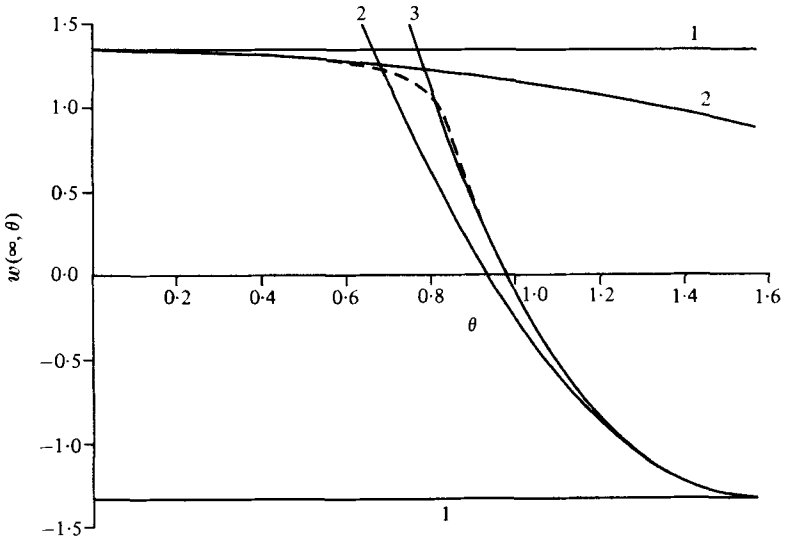

FIGURE 3. The variation of $w(\infty, \theta)$ as a function of θ. The numbers 1, 2 and 3 indicate the number of terms used in (28).

according to the solution in the form of (25) and (24) respectively. For $\theta = \frac{9}{20}\pi$ the analytical and numerical results are indistinguishable graphically, and therefore only the numerical results are shown in figure 5(*a*). The results for the other two components of velocity can be obtained with a similar degree of agreement. Hence it has been shown that the terminal solutions predicted by the theory are being approached without the necessity of enforcing them as boundary conditions. It has moreover been shown that a steady-state boundary-layer solution of the type envisaged by Stewartson (1957) is approached. The steady-state model is probably not realizable in practice. It nevertheless derives from a solution of the boundary-layer equations (11)–(13); and the local solutions near $\theta = 0$ and $\theta = \pi$ are consistent with the solution for all θ. The question of how the boundary-layer model relates to the actual situation still remains an open question, but we now show that the steady-state model is also consistent with the limit for large time of the solution of the time-dependent boundary-layer equations.

4. Impulsively stopped rotating sphere in a rotating fluid

Dennis & Ingham (1979) investigated the motion of a viscous incompressible fluid that occupies the region outside a sphere that at time $t = 0$ is impulsively started to rotate with an angular velocity ω_0 about an axis through its centre. In the present paper the inverse of this problem is considered, namely the sudden stopping of the sphere after it has been rotating with the fluid with a constant angular velocity ω_0 about an axis through a diameter of the sphere. The unsteady boundary-layer equations are assumed to hold. The basic equations and analysis are virtually the same as that presented by Dennis & Ingham (1979); we therefore give only a brief summary here.

Owing to the impulsive nature of the motion a boundary layer of thickness

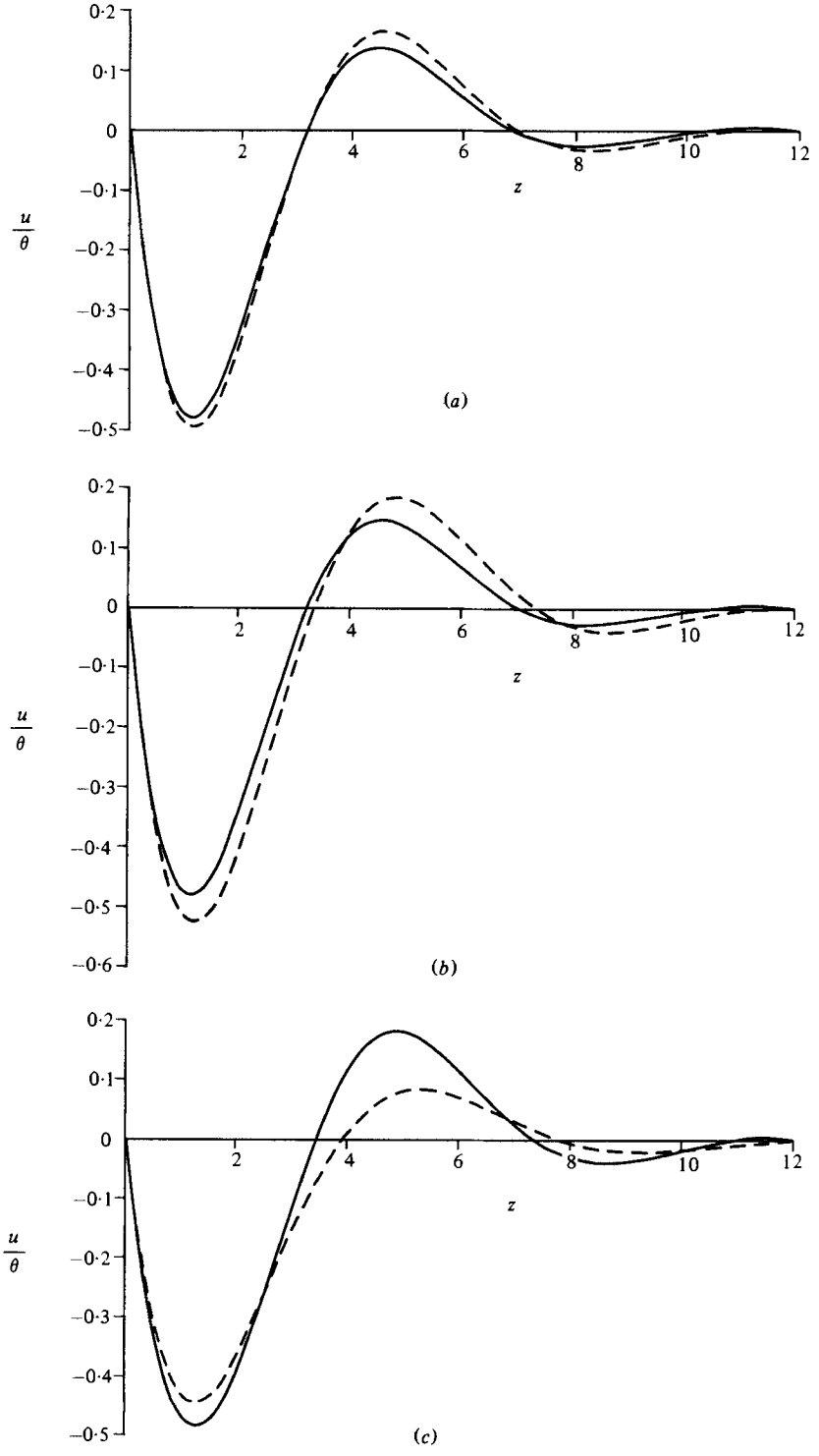

FIGURE 4(*a–c*). For caption see facing page.

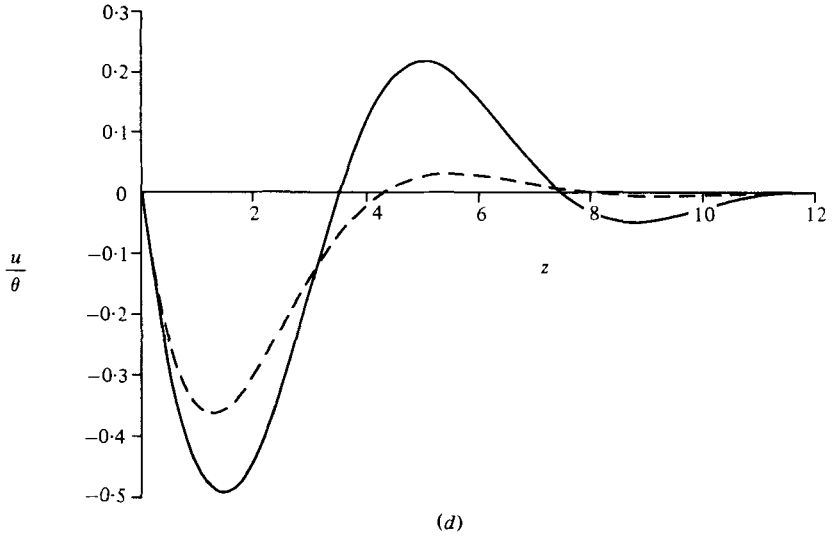

FIGURE 4. The variation of u/θ as a function of z; solid line using the two term expansion in (25), broken line the numerical solution: (*a*) $\theta = \frac{1}{20}\pi$; (*b*) $\frac{1}{10}\pi$; (*c*) $\frac{1}{5}\pi$; (*d*) $\frac{1}{4}\pi$.

proportional to $(t/R)^{\frac{1}{2}}$ is initially formed on the surface of the sphere. Thus the co-ordinate normal to the surface of the sphere is taken as

$$x = \tfrac{1}{2}(t/R)^{-\frac{1}{2}}(r-1) \tag{29}$$

in the initial stages of the motion. The method of solution is the series-truncation procedure employed by Dennis & Ingham (1979) in which the dependent variables are expressed as series of Gegenbauer functions in the θ-direction. In theory the series are infinite, but in practice they are each truncated to a finite number n_0 of terms. Initially the nature of the motion is such that n_0 need only be small to give an accurate description of the flow, and at the start $n_0 = 2$ was assigned. The rapid variation of the flow for small t was dealt with by taking 25 small time steps of magnitude 0·001, and the process was continued with 159 time steps of size 0·025. Accuracy checks were applied periodically by obtaining solutions with both half and double the current time step. Comparison of these solutions was satisfactory, as also were similar comparisons of solutions obtained using grid sizes of 0·05 and 0·1 in the x-direction. The finite value $x = x_m$ at which the outer boundary conditions were assumed to hold was varied at different times to ensure that it was large enough; at small times $x_m = 5$ was satisfactory.

The effect of the sudden stopping of the sphere gradually diffuses outwards into the surrounding fluid with increasing time. The flow becomes more complicated and more terms become necessary in the series of Gegenbauer functions. This is accommodated by increasing n_0 by one as each new term becomes significant. In this way the step-by-step integration was continued up to $t = 4$, by which time the value $n_0 = 16$ had been reached. For $t > 4$ the integration of the unsteady boundary-layer equations was continued using variables appropriate to the steady-state boundary layer and with $n_0 = 20$, which was the greatest value consistent with limitations on computer storage. The integration up to $t = 20$ was carried out using a time step of magnitude 0·1. After $t = 20$ the time step was increased to 0·5 and the integration

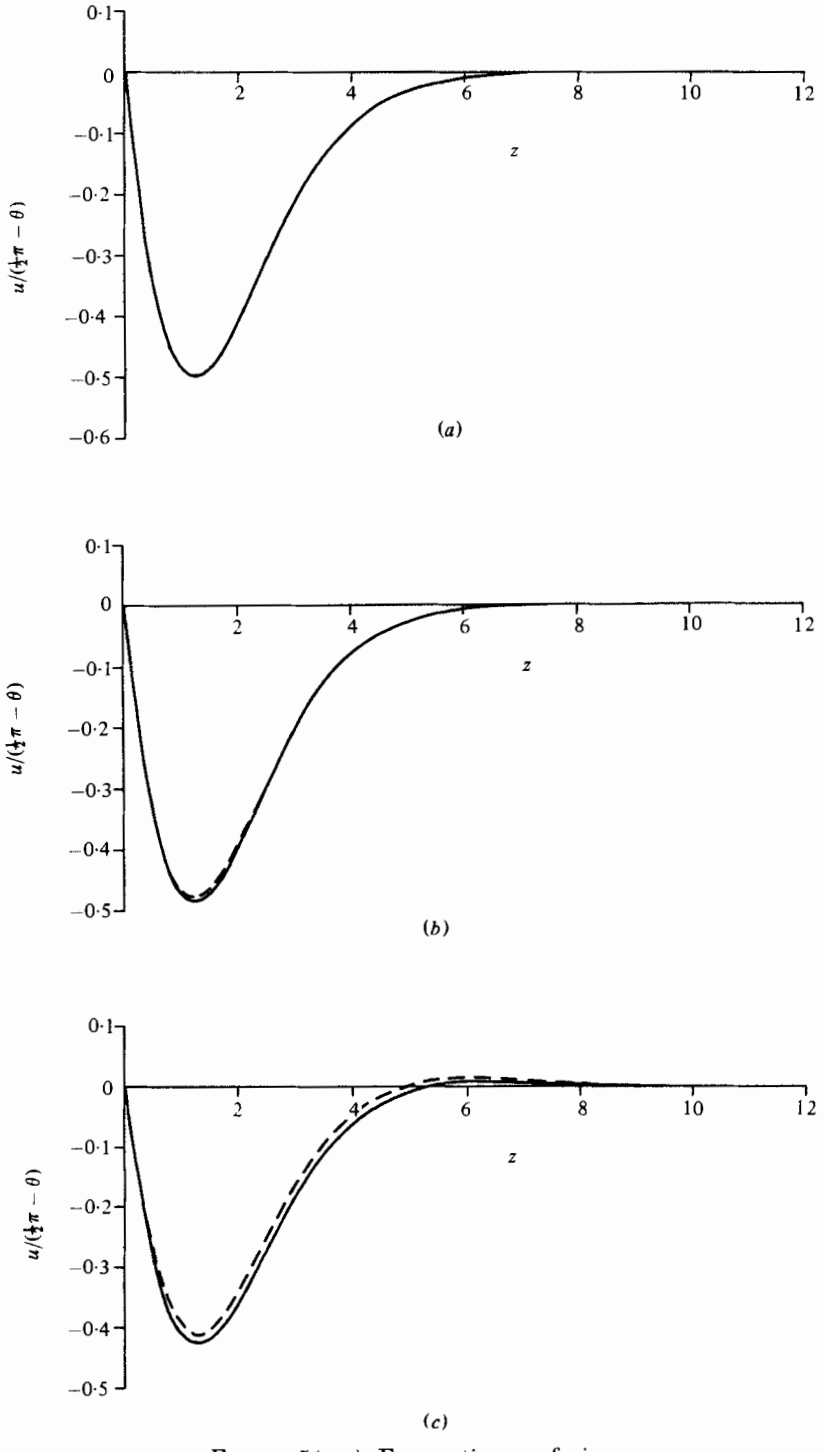

FIGURE 5(*a*–*c*). For caption see facing page.

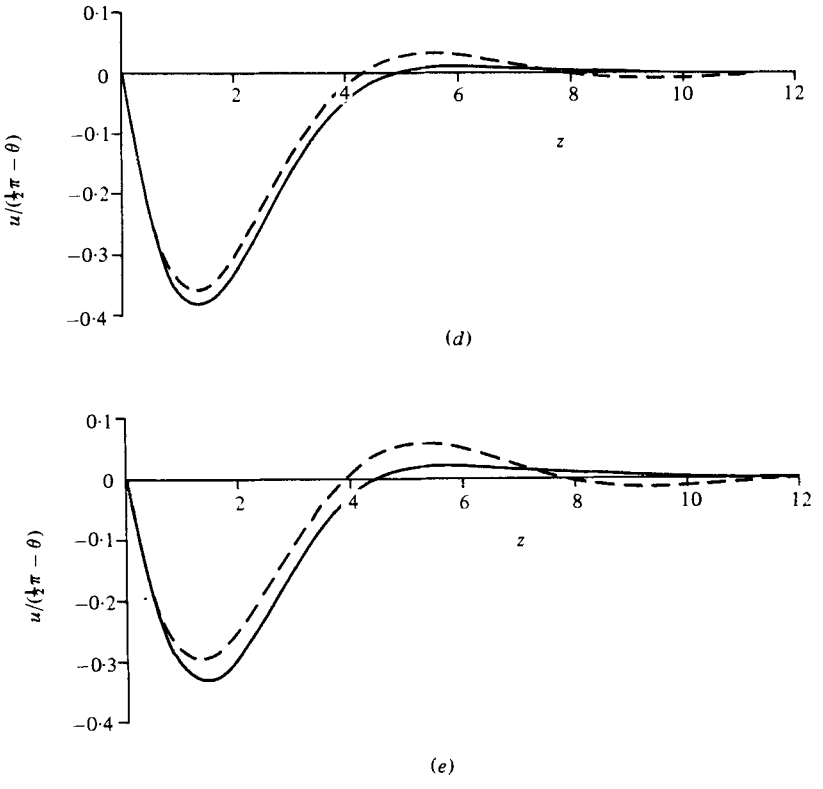

FIGURE 5. The variation of $u/(\frac{1}{2}\pi-\theta)$ as a function of z; solid line using the three-term expansion in (24), broken line the numerical solution: (*a*) $\theta = \frac{9}{20}\pi$; (*b*) $\frac{2}{5}\pi$; (*c*) $\frac{3}{10}\pi$; (*d*) $\frac{1}{4}\pi$; (*e*) $\frac{1}{5}\pi$.

extended to $t = 300$. Because of the larger time steps and limitation on n_0, the accuracy deteriorates for $t > 4$, but the main aim was to investigate whether a steady-state solution appeared to be approached. The location $z = z_\infty$, of the outer boundary was taken at the same station $z_\infty = 60$ used by Bodonyi (1978), although Banks & Zaturska (1979) suggest that this is too small for accurate results.

Near the poles of the sphere the time development of the flow has been investigated by Bodonyi (1978) and Banks & Zaturska (1979). With

$$u = \theta f_0(z,t), \quad v = \theta g_0(z,t), \quad w = h_0(z,t) \tag{30}$$

the unsteady boundary-layer equations give rise to the equations

$$\left.\begin{aligned} \frac{\partial f_0}{\partial t} + f_0^2 + h_0\frac{\partial f_0}{\partial z} - g_0^2 &= \frac{\partial^2 f_0}{\partial z^2} - 1, \\ \frac{\partial g_0}{\partial t} + h_0\frac{\partial g_0}{\partial z} + 2f_0 g_0 &= \frac{\partial^2 g_0}{\partial z^2}, \\ 2f_0 + \frac{\partial h_0}{\partial z} &= 0. \end{aligned}\right\} \tag{31}$$

If the sphere has been stopped impulsively, the initial and boundary conditions are

$$\left.\begin{aligned} &h_0 = f_0 = 0, \quad g_0 = 1 \quad (t = 0, \quad \text{all} \quad z), \\ &g_0 \to 1, \quad f_0 \to 0 \quad (z \to \infty, \quad \text{all} \quad t), \\ &g_0 = 0, \quad h_0 = f_0 = 0 \quad (z = 0, \quad \text{all} \quad t > 0). \end{aligned}\right\} \tag{32}$$

Equations (31) subject to the conditions (32) have been solved in the present paper using the method described by Banks & Zaturska (1979).

Near the equator we write

$$u = (\theta - \tfrac{1}{2}\pi) f_1(z,t), \quad v = g_1(z,t), \quad w = h_1(z,t), \tag{33}$$

and then the unsteady boundary-layer equations give

$$\left.\begin{aligned} \frac{\partial f_1}{\partial t} + f_1^2 + h_1 \frac{\partial f_1}{\partial z} + g_1^2 &= \frac{\partial^2 f_1}{\partial z^2} + 1, \\ \frac{\partial g_1}{\partial t} + h_1 \frac{\partial g_1}{\partial z} &= \frac{\partial^2 g_1}{\partial z^2}, \\ f_1 + \frac{\partial h_1}{\partial z} &= 0. \end{aligned}\right\} \tag{34}$$

If the sphere has been stopped impulsively the initial and boundary conditions are

$$\left.\begin{aligned} &h_1 = f_1 = 0, \quad g_1 = 1 \quad (t = 0, \quad \text{all} \quad z), \\ &g_1 \to 1, \quad f_1 \to 0 \quad (z \to \infty, \quad \text{all} \quad t), \\ &g_1 = 0, \quad h_1 = f_1 = 0 \quad (z = 0, \quad \text{all} \quad t > 0). \end{aligned}\right\} \tag{35}$$

Equations (34), subject to the conditions (35), have been solved numerically in exactly the same manner as the equations (31) subject to the conditions (32). The object was to see if the steady-state solution was approached at both $\theta = 0$ and $\frac{1}{2}\pi$. It was found that near the pole the approach to the steady state was extremely slow and that all quantities oscillated about their steady-state values. The results obtained are in good agreement with Banks & Zaturska (1979) and to a lesser extent with Bodonyi (1978). Thus the detailed results are not presented, but the agreement served as a check on the accuracy of the method for dealing with the unsteady boundary-layer equations at the equator, namely (34).

Figure 6 shows the approach to the steady-state solution for the skin-friction coefficients $R^{-\frac{1}{2}}(\partial u/\partial r)_{r=1,\,\theta=\frac{1}{2}\pi}$, $R^{-\frac{1}{2}}(\partial v/\partial r)_{r=1,\,\theta=\frac{1}{2}\pi}$ and for $w(\infty, \frac{1}{2}\pi, t)$. A similarity solution in powers of t can be obtained, in the usual manner, for the initial variation of the flow. Thus as $t \to 0$ we can take

$$\left.\begin{aligned} \eta &= z/(2t^{\frac{1}{2}}), \\ f_1(z,t) \sim t f_1^*(\eta), \quad g_1(z,t) &\sim g_1^*(\eta), \quad h_1(z,t) = t^{\frac{3}{2}} h_1^*(\eta). \end{aligned}\right\} \tag{36}$$

From (34) the differential equations satisfied by f_1^*, g_1^* and h_1^* become

$$\left.\begin{aligned} \frac{d^2 f_1^*}{d\eta^2} + 2\eta \frac{df_1^*}{d\eta} - 4f_1^* + 4(1 - g_1^{*2}) &= 0, \\ \frac{d^2 g_1^*}{d\eta^2} + 2\eta \frac{dg_1^*}{d\eta} &= 0, \\ \frac{dh_1^*}{d\eta} + 2f_1^* &= 0. \end{aligned}\right\} \tag{37}$$

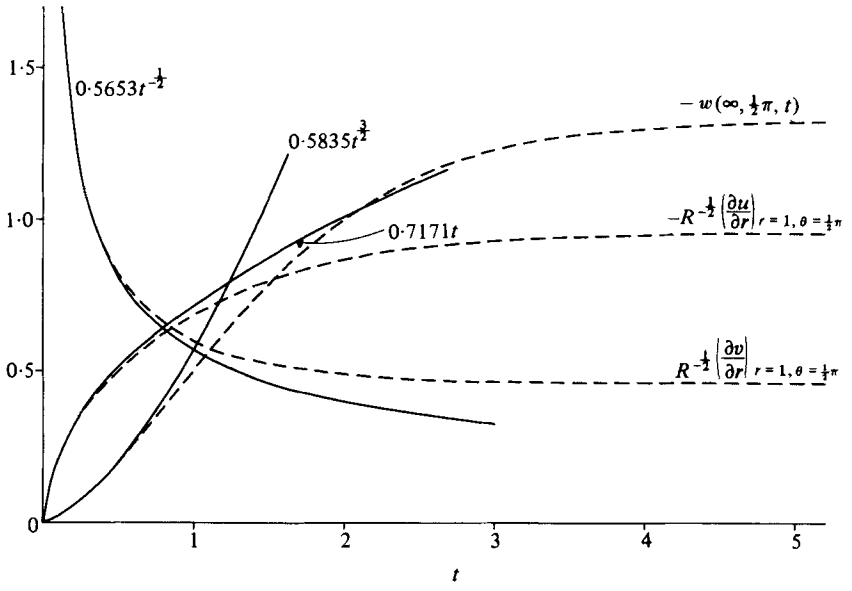

FIGURE 6. The variation of $R^{-\frac{1}{2}}(\partial u/\partial r)_{r=1, \theta=\frac{1}{2}\pi}$, $R^{-\frac{1}{2}}(\partial v/\partial r)_{r=1, \theta=\frac{1}{2}\pi}$ and $w(\infty, \pi/2, t)$ as functions of time. Solid lines: analytical results as given in equation (39). Broken lines: numerical results.

The boundary conditions (32) reduce to

$$\left.\begin{aligned} &f_1^* = h_1^* = g_1^*(0) = 0, \\ &f_1^* \to 0, \quad g_1^* \to 1 \quad (\eta \to \infty). \end{aligned}\right\} \tag{38}$$

Equations (37) have been solved subject to the boundary conditions (38), and this gives, for small values of t,

$$\left.\begin{aligned} R^{-\frac{1}{2}}(\partial u/\partial r)_{r=1, \theta=\frac{1}{2}\pi} &\sim -0{\cdot}7171t^{\frac{1}{2}}, \\ R^{-\frac{1}{2}}(\partial v/\partial r)_{r=1, \theta=\frac{1}{2}\pi} &\sim 0{\cdot}5653t^{-\frac{1}{2}}, \\ w(\infty, \tfrac{1}{2}\pi, t) &\sim -0{\cdot}5835t^{\frac{3}{2}}. \end{aligned}\right\} \tag{39}$$

Results according to (39) are also shown in figure 6, and the full numerical solution is in good agreement with these results. Figure 7 shows the time development of the function $f_1(z, t)$ in (33). The results for the other components of velocity show similar approaches to their steady-state values and are therefore not presented. It is seen that the flow approaches the steady state at the equator very rapidly, which is in direct contrast to the approach to the steady state at the pole.

Results from the integration of the unsteady boundary-layer equations by the series-truncation method are shown in figures 8, 9 and 10, which give the time variation of $R^{-\frac{1}{2}}(\partial u/\partial r)_{r=1}$, $R^{-\frac{1}{2}}(\partial v/\partial r)_{r=1}$ and $w(\infty, \theta, t)$ respectively. Also shown are the corresponding steady-state solutions. It is seen that the solution approaches the steady state faster near the equator than at the poles. When $t = 4$ the solution near the equator has almost reached its steady-state situation, whereas it requires $t \sim 300$ before the flow near the pole approaches its steady-state value. The details of the approach to the steady state near the poles are qualitatively similar to those

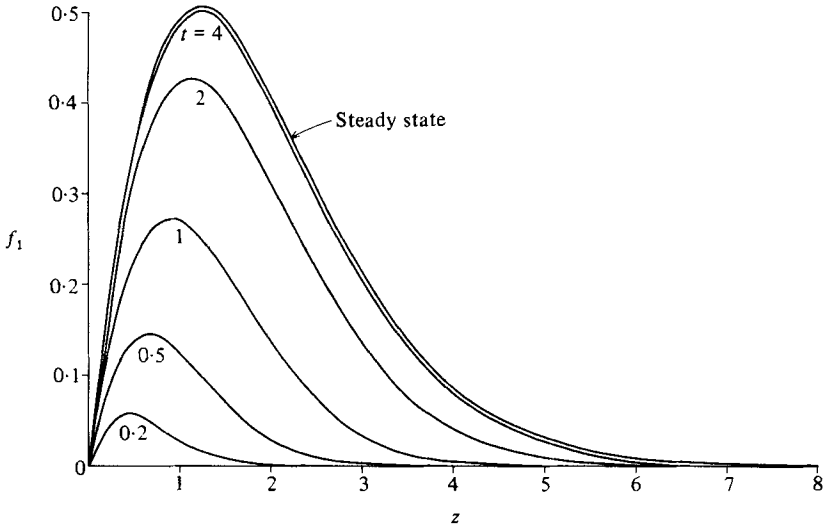

FIGURE 7. The variation of $f_1(z, t)$ in (33) as a function of time.

presented by Bodonyi (1978) and Banks & Zaturska (1979). The radial velocity at the outer edge of the boundary layer shows a chaotic behaviour for $0 < \theta < \frac{1}{4}\pi$. This is consistent with the results of Banks & Zaturska (1979), who show that at the pole the radial velocity oscillates with time at large values of the time. Thus, if at the equator the steady state has been approached and one takes a time when the radial velocity at the pole is negative then, by continuity, we require a large positive radial velocity to be generated somewhere between $\theta = 0$ and $\theta = \frac{1}{2}\pi$. This can be seen in figure 10 at $t = 4$; it occurs also at later times, but we do not consider the results accurate enough to be presented in detail.

In conclusion it has been shown that a steady-state boundary-layer solution does exist for the flow near a fixed sphere with the fluid outside the sphere rotating as a solid body. Since it is doubtful whether physically this solution can exist, an unsteady numerical approach has been investigated. This showed that the approach to the terminal solution near the equator was very rapid, whereas near the pole it was approached, but much more slowly. The series-truncation method showed that the steady-state solution appeared to be approached for all values of θ, although again the approach was much faster near the equator than the pole. It has not been possible to obtain with uniform accuracy all quantities for larger values of the time. This applies particularly to $w(\infty, \theta, t)$, especially in the region $0 < \theta < \frac{1}{4}\pi$, where the behaviour is chaotic. It is possible that the limitations on the various parameters, in particular z_∞, imposed by computer storage may have a bearing on this situation.

The computations were carried out on the Amdahl computer at the University of Leeds. The work forms part of a general project supported by grants from the Natural Sciences and Engineering Research Council of Canada and by NATO.

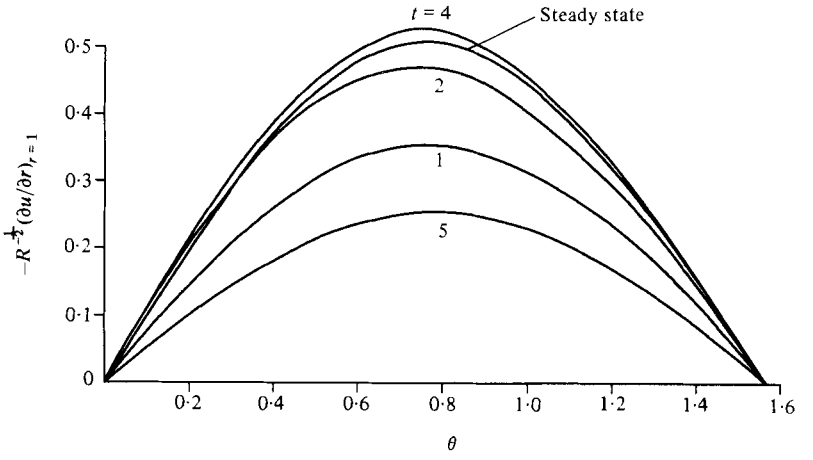

FIGURE 8. The variation of $R^{-\frac{1}{2}}(\partial u/\partial r)_{r=1}$ as a function of θ at various times.

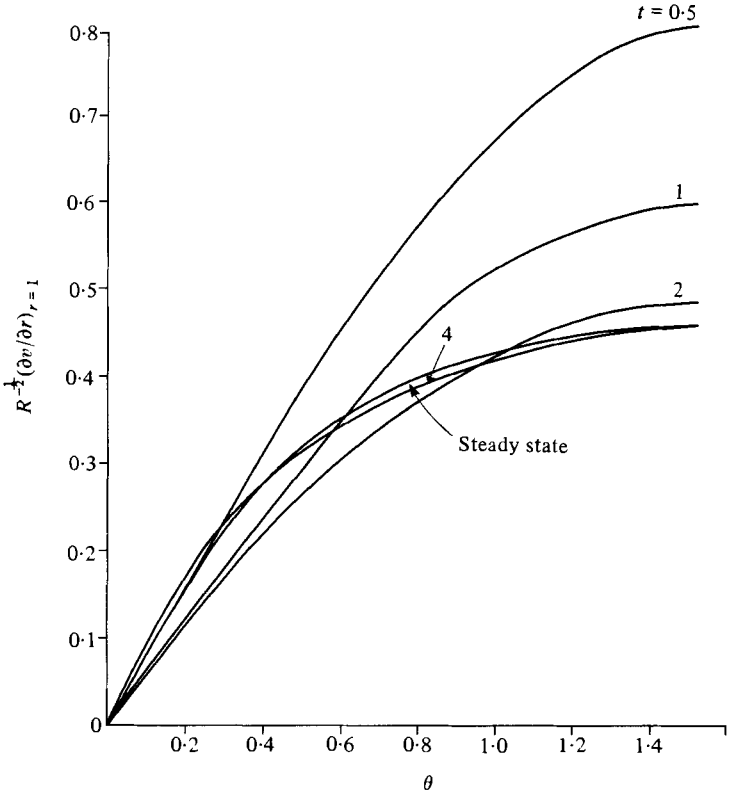

FIGURE 9. The variation of $R^{-\frac{1}{2}}(\partial v/\partial r)_{r=1}$ as a function of θ at various times.

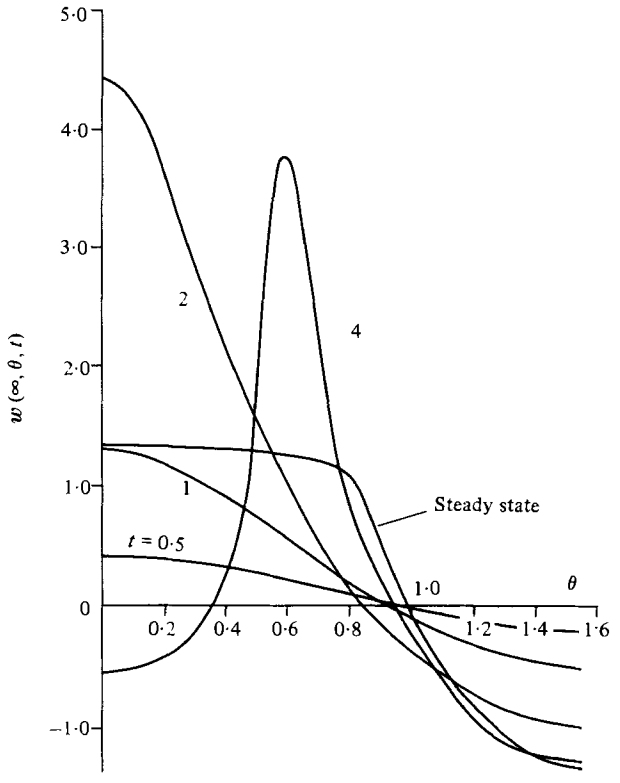

FIGURE 10. The variation of $w(\infty, \theta, t)$ as a function of θ at various times.

REFERENCES

ANDERSON, O. L. 1966 Ph.D. thesis, Rensselaer Polytechnic Institute.
BANKS, W. H. H. 1971 *Acta Mech.* **11**, 27.
BANKS, W. H. H. 1976 *Acta Mech.* **24**, 273.
BANKS, W. H. H. & ZATURSKA, M. B. 1979 *A.I.A.A. J.* **17**, 1263.
BELCHER, R. J., BURGGRAF, O. R. & STEWARTSON, K. 1972 *J. Fluid Mech.* **52**, 753.
BÖDEWADT, U. T. 1940 *Z. angew. Math. Mech.* **20**, 241.
BODONYI, R. J. 1978 *Q. J. Mech. Appl. Math.* **31**, 461.
BOWDEN, F. P. & LORD, R. G. 1963 *Proc. R. Soc. Lond.* A **271**, 143.
BURGGRAF, O. R., STEWARTSON, K. & BELCHER, R. 1971 *Phys. Fluids* **14**, 1821.
COOKE, J. C. 1966 *Royal Aircraft Establishment Tech. Rep. no.* 66–128.
DENNIS, S. C. R. 1972 *J. Inst. Math. Applics* **10**, 105.
DENNIS, S. C. R. & INGHAM, D. B. 1979 *Phys. Fluids* **22**, 1.
DENNIS, S. C. R., INGHAM, D. B. & SINGH, S. N. 1981 *Q. J. Mech. Appl. Math.* **34**, 361.
HALL, M. G. 1969 *Proc. R. Soc. Lond.* A **310**, 400.
HOWARTH, L. 1951 *Phil. Mag.* **42**, 1308.
INGHAM, D. B. 1978 *Phys. Fluids* **21**, 1891.
MOORE, F. K. 1956 *Adv. Appl. Mech.* **4**, 159.
RICHARDSON, P. D. 1976 *Int. J. Heat Mass Transfer* **19**, 1189.
RILEY, N. 1962 *Q. J. Mech. Appl. Math.* **15**, 435.
SAWATZKI, O. 1970 *Acta Mech.* **9**, 159.
SCHULTZ-GRÜNOW, F. 1935 *Z. angew. Math. Mech.* **15**, 191.
SMITH, F. T. 1975 *J. Fluid Mech.* **71**, 15.
SMITH, F. T. & DUCK, P. W. 1977 *Q. J. Mech. Appl. Math.* **30**, 143.
STEWARTSON, K. 1957 In *Boundary Layer Research*, p. 59. Springer.
TAKAGI, H. 1977 *J. Phys. Soc. Japan* **42**, 319.